Supplementary Information

A Mouse Model for MERS Coronavirus Induced Acute Respiratory Distress Syndrome

Adam S. Cockrell, Boyd L. Yount, Trevor Scobey, Kara Jensen, Madeline Douglas, Anne Beall, Xian-Chun Tang, Wayne A. Marasco, Mark T. Heise, Ralph S. Baric

Address Correspondence: R.S.B. (rbaric@email.unc.edu)

Supplementary Table 1

Supplementary Figures 1-14

Supplementary Table 1

Guide RNAs and oligo sequences to humanize the alleles encoding amino acids 288 and 330 in mouse DPP4

Edited Amino Acid	Cas 9 Guide Sequence	Oligo for Homology Directed Repair
A288L	5’-GCTCCTGCATCTGTGGCAAG-3’	5’-TCAGCTCATCCTCTAGTGCGGCTCCCATCCAAATCCCTGCTCCTGCATCTGTGTTGAGAGGGTAAGATGCTCTACCTGAGTGCTTGGGTGTAGATCGCTTTCCACTAC-3’
T330R	5’-ATGATAAGATCAACCTAACG-3’	5’-GATTCAGAACTATTCCGTGATGGCTATCTGTGACTATGATAAGATCAACCTAAGATGGAACTGTCCATCCGTAAGATTTCCCTGGGATGCTCTGCTGTTCCAACAGCA-3’

Supplementary Figure 1

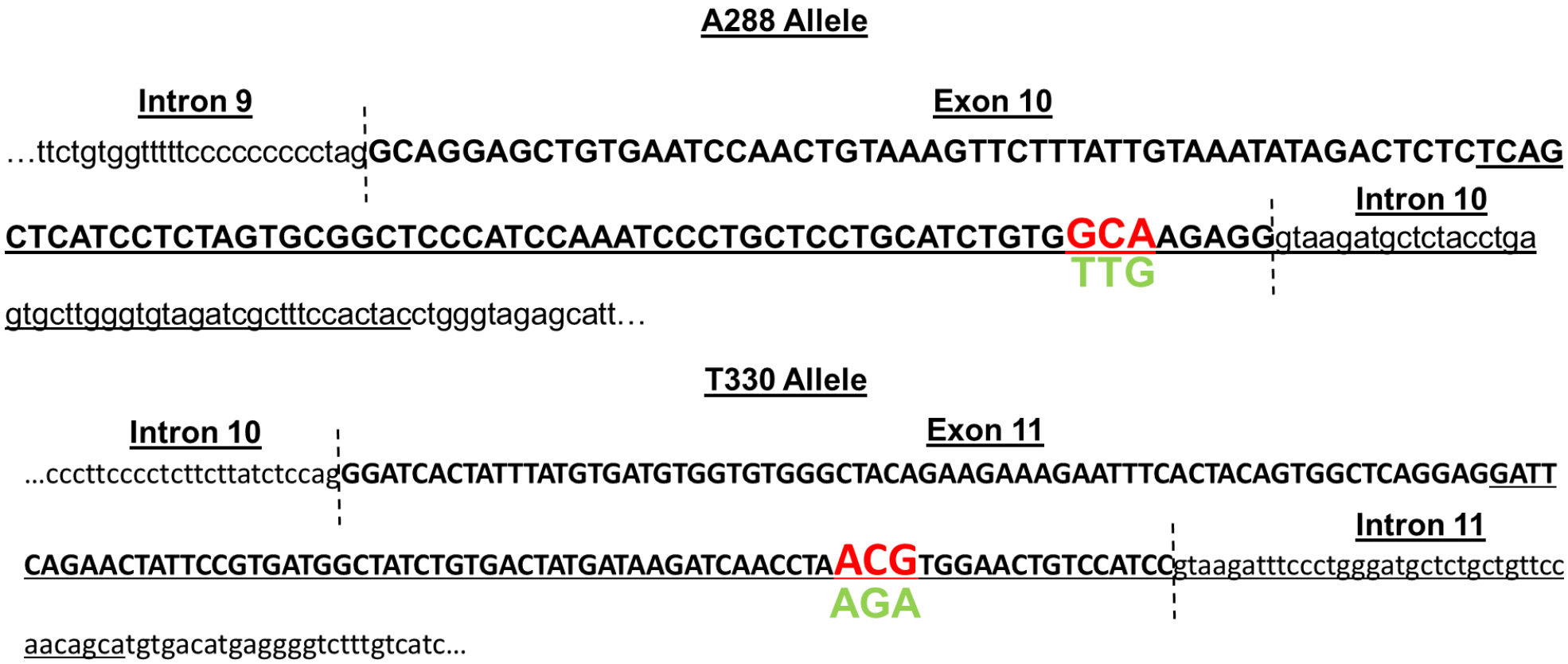

Supplementary Figure 1. Mouse DPP4 288 and 330 alleles modified by CRISPR/Cas9. Mouse alleles encoding A288 and T330 (red) are shown on exon 10 and 11 of mDPP4, respectively. Underlined regions indicate sequence encoded in oligo's for homology-directed repair with CRISPR/Cas9 to introduce the modified nucleotides (green). Vertical hashes indicate intron/exon borders.

Supplementary Figure 2

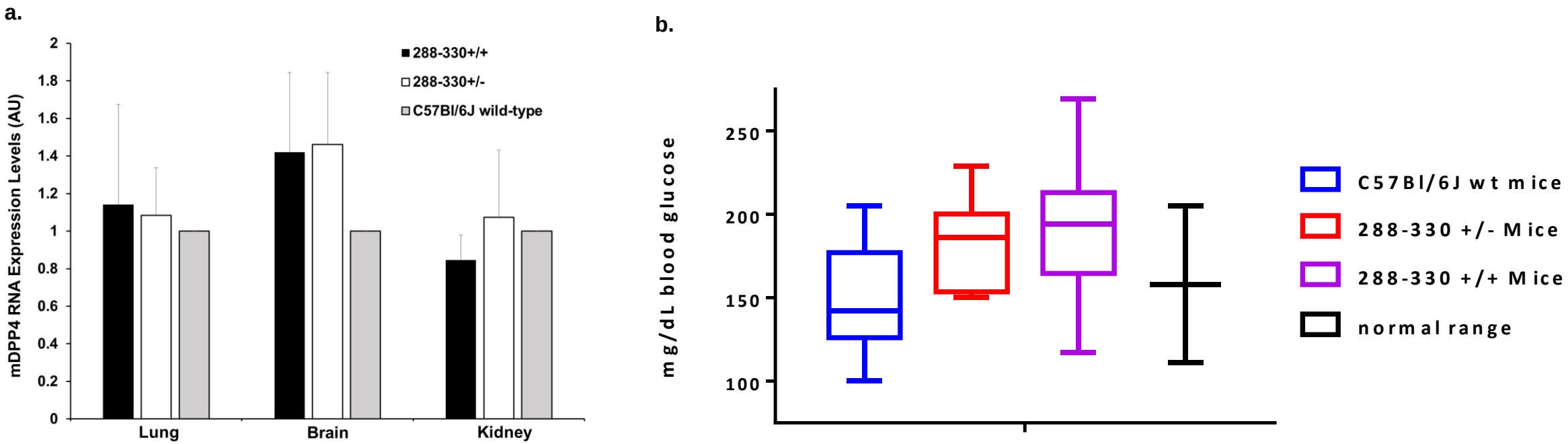

Supplementary Figure 2. Bio-distribution and functional characterization of modified mouse DPP4. (a) RT-qPCR was used to evaluate the mRNA levels of mDPP4 in the lungs, brain, and kidneys of 288-330$^{+/+}$ (*n* = 5) and 288-330$^{+/-}$ (*n* = 5) compared with C57Bl/6J wild-type mice (*n* = 5). Values are expressed as arbitrary units that were normalized to 18S ribosomal RNA and C57Bl/6J wild-type mouse samples using the equation $2^{-\Delta\Delta Cp}$. Error bars are +SD. (b) Blood glucose levels were measure from whole blood samples of 288-330$^{+/+}$ (*n* = 16), 288-330$^{+/-}$ (*n* = 14), and C57Bl/6J wild-type mice (*n* = 15). Values are compared to the anticipated normal range for mice. Error bars are +/- SD.

Supplementary Figure 3

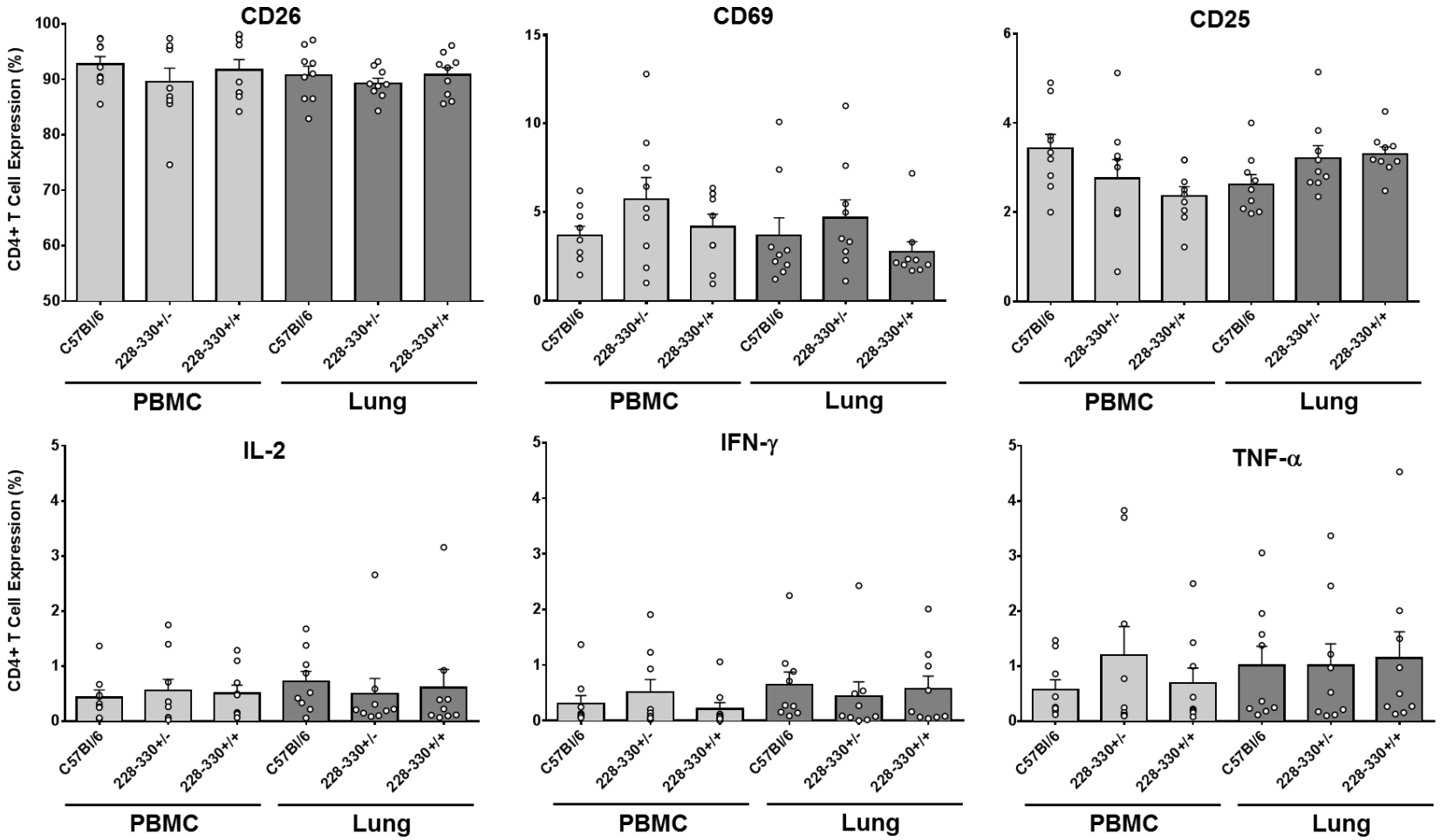

Supplementary Figure 3. Modification of mDPP4 does not alter activation profiles of CD4+ T cells. Lymphocytes from peripheral blood mononuclear cells (PBMCs) and lungs of C57Bl/6J wild-type (*n* = 9), 288-330$^{+/-}$ (*n* = 9), and 288-330$^{+/+}$ (*n* = 9) were analyzed by flow cytometry. The percent of CD4+ T cells were assessed for expression of mouse DPP4 (CD26), CD69, CD25, IL-2, IFNg, and TNF-a. Error bars are +SD.

Supplementary Figure 4

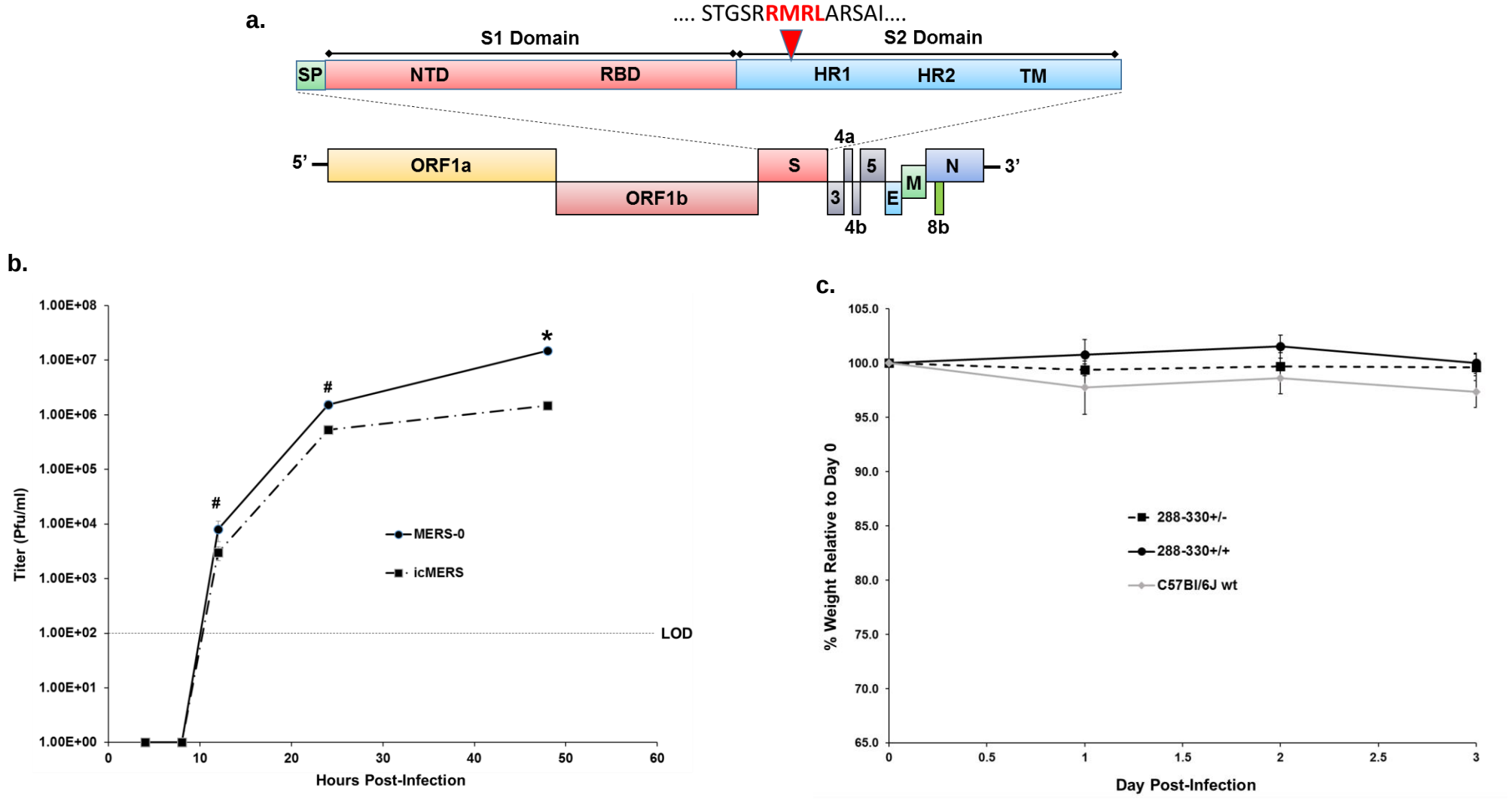

Supplementary Figure 4. MERS-0 replicates to high titer *in vitro*, but causes no disease. (a) Cartoon of MERS-CoV with an expanded view of the spike protein showing the amino acid changes in the S2 domain (red). (b) Growth curves on Vero81 cells of MERS-0 (n = 3) compared to the MERS-CoV infectious clone (icMERS) (n = 3). Student t-test was used to compare titers at indicated time points (# = $p < 0.05$, and * = $p < 0.01$). (c) MERS-0 does not cause weight loss in 288-330$^{+/-}$ (n = 4) or 288-330$^{+/+}$ (n = 4) mice. Error bars are +/- SD.

Supplementary Figure 5

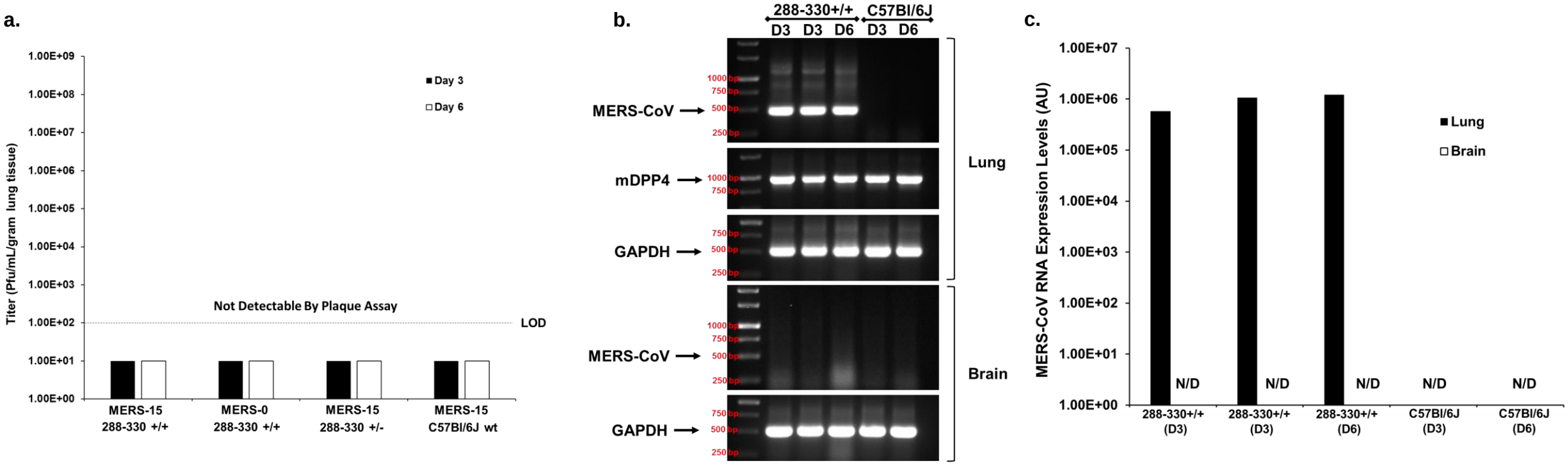

Supplementary Figure 5. Mouse-adapted MERS-15 virus does not infect the brain. (a) Viral titers from brain tissue were determined by plaque assays at day 3 and 6 p.i. for 288-330$^{+/+}$ + MERS-15 (day 3, *n* = 4 and day 6, *n* = 4), or MERS-0 (day 3, *n* = 4 and day 6, *n* = 4); 288-330$^{+/-}$ + MERS-15 (day 3, *n* = 4 and day 6 *n* = 4); and, C57Bl/6J wt + MERS-15 (day 3, *n* = 4 and day 6, *n* = 3). The limit of detection (LOD) is indicated. (b) Lung and brain RNA was examined by RT-PCR to determine if MERS-15 RNA could be detected in the lung and brains of 288-330$^{+/+}$ and C57Bl/6J wt mice at days 3 and 6 p.i. Mouse DPP4 and GAPDH were examined as controls (bp = base pair size markers in red). (c) RT-qPCR was used to evaluate the mRNA levels of mDPP4 in the lungs and brains of MERS-15 infected 288-330$^{+/+}$ and C57Bl/6J wild-type mice shown in (b). Values are expressed as arbitrary units that were normalized to 18S ribosomal RNA and C57Bl/6J wild-type mouse samples using the equation $2^{-\Delta\Delta Cp}$. N/D indicates none detected.

Supplementary Figure 6

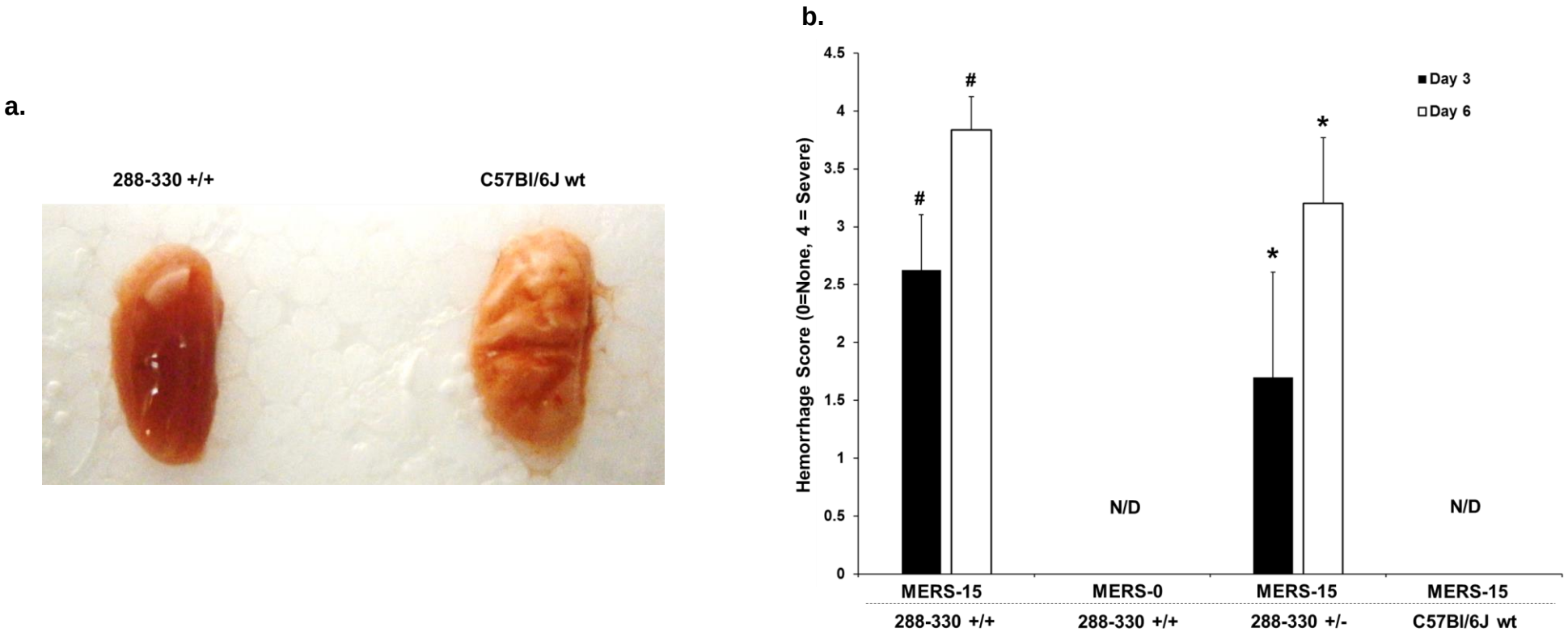

Supplementary Figure 6. Mouse-adapted MERS-15 cause's hemorrhage in mouse lungs. (a) Image of a hemorrhaged left lung lobe from a 288-330$^{+/+}$ mouse infected with MERS-15 (left) compared to left lung lobe of a C57Bl/6J wt mouse infected with MERS-15 (right). Image is representative of at least 3 lungs. (b) The severity of hemorrhage was scored for 288-330$^{+/+}$ + MERS-15 (day 3, n = 4 and day 6, n = 3), or MERS-0 (day 3, n = 5 and day 6, n = 5); 288-330$^{+/-}$ + MERS-15 (day 3, n = 5 and day 6, n = 5); and, C57Bl/6J wt + MERS-15 (day 3, n = 5 and day 6, n = 5). Lungs were scored from 0 (no hemorrhage) to 4 (severe hemorrhaging in all lobes of the lung). N/D is none detectable. Student t-test was used to demonstrate significant differences between days 3 and 6 p.i. for 288-330$^{+/+}$ (# is $p < 0.05$) and 288-330$^{+/-}$ (* is $p < 0.05$) mice infected with MERS-15. Error bars are +SD.

Supplementary Figure 7

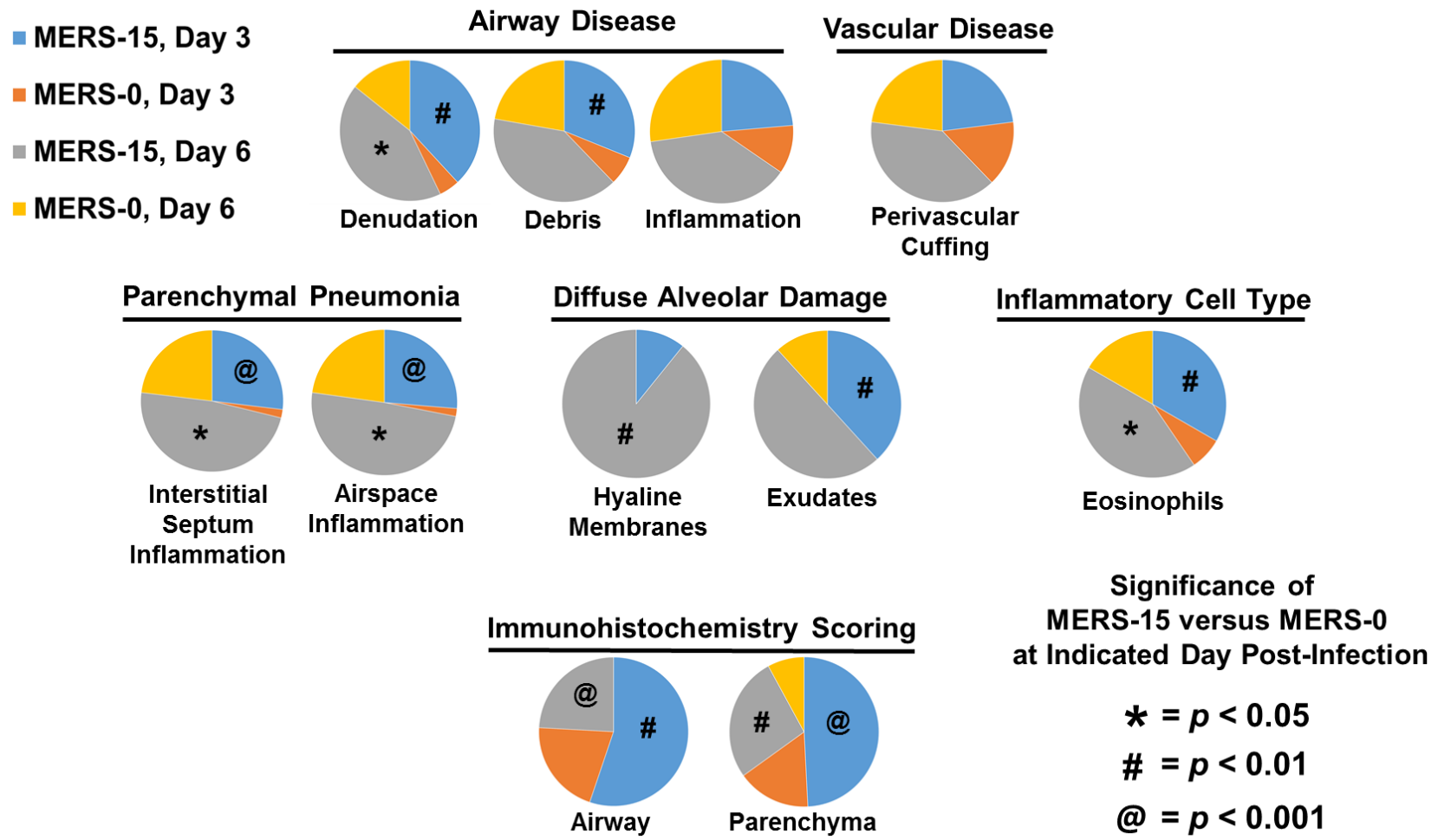

Supplementary Figure 7. Quantitation of histopathological findings for MERS-15 compared to MERS-0 at Days 3 and 6 post-infection. Data are represented as pie graphs with MERS-15/Day 3 (blue), MERS-0/Day 3 (orange), MERS-15/Day 6 (gray), and MERS-0/Day 6 (yellow). Each indication was scored, blinded on a scale of 0 – 3, where 0 = none, 1 = mild, 2 = moderate, and 3 = severe. Average scores are represented on the pie graphs with significance indicated by * = $p < 0.05$; # = $p < 0.01$; and @ = $p < 0.001$. Student *t*-test was used to compare the respective indication at days 3 and 6 p.i. for 288-330$^{+/+}$ mice infected with MERS-15 (day 3, $n = 5$ and day 6, $n = 5$) compared to those infected with MERS-0 (day 3, $n = 5$ and day 6, $n = 5$).

Supplementary Figure 8

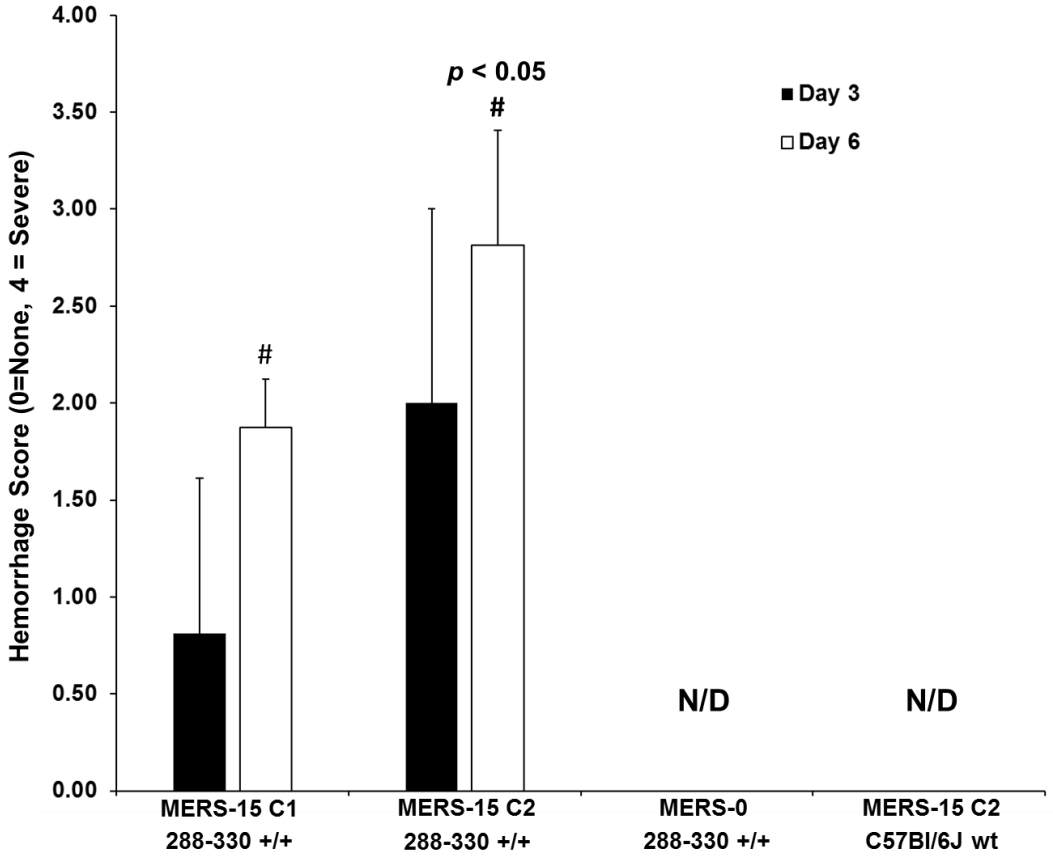

Supplementary Figure 8. Mouse-adapted MERS-15 clone 2 causes more severe hemorrhage than MERS-15 clone 1. Severity of hemorrhage was scored for 288-330$^{+/+}$ + MERS-15 C1 (day 3, *n* = 4 and day 6, *n* = 4), MERS-15 C2 (day 3, *n* = 3 and day 6, *n* = 7), or MERS-0 (day 3, *n* = 3 and day 6, *n* = 3); and, C57Bl/6J wt + MERS-15 C2 (day 3, *n* = 3 and day 6, *n* = 3). Lung hemorrhage was scored at day 3 and day 6 p.i. Lungs are given a score from 0 (no hemorrhage) to 4 (severe hemorrhaging in all lobes of the lung). N/D is none detectable. Student *t*-test was used to compare hemorrhage scores at day 6 post-infection for 288-330$^{+/+}$ + MERS-15 C1, and MERS-15 C2 (# is $p < 0.05$). Error bars are +SD.

Supplementary Figure 9

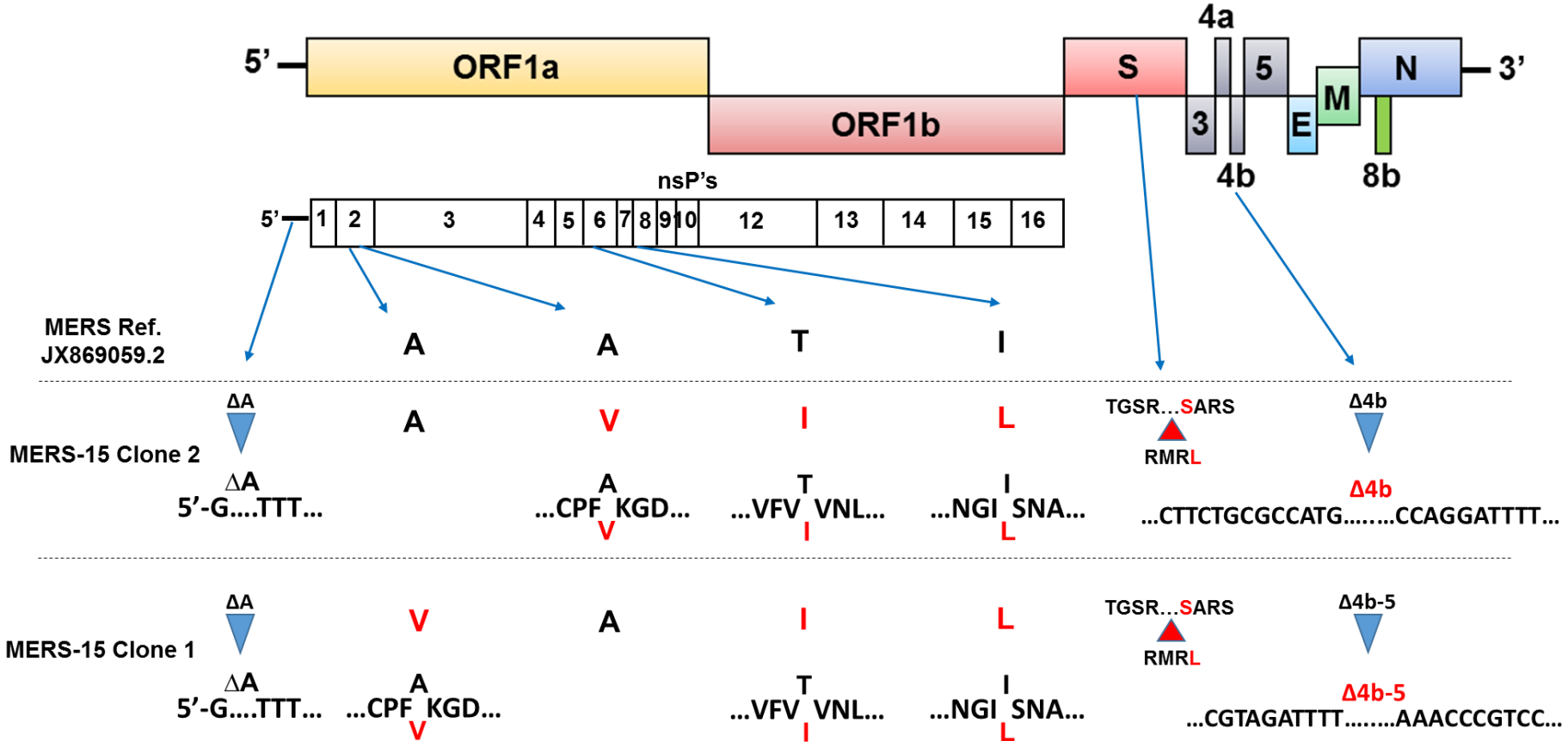

Supplementary Figure 9. Mutations identified in MERS-15 clone 2 and MERS-15 clone 1 compared to the MERS-CoV reference sequence, JX869059.2. A deletion of the second nucleotide in the 5'UTR is shown with a blue arrow head. Amino acid changes in nsP2, nsP6, and nsP8 are shown in red. The original RMR insertion with the S to L change in the S2 domain of the spike protein with the red arrow head. A deletion in the accessory gene Orf4b is shown with the blue arrow head with the sequence encoding the borders of the deletion shown.

Supplementary Figure 10

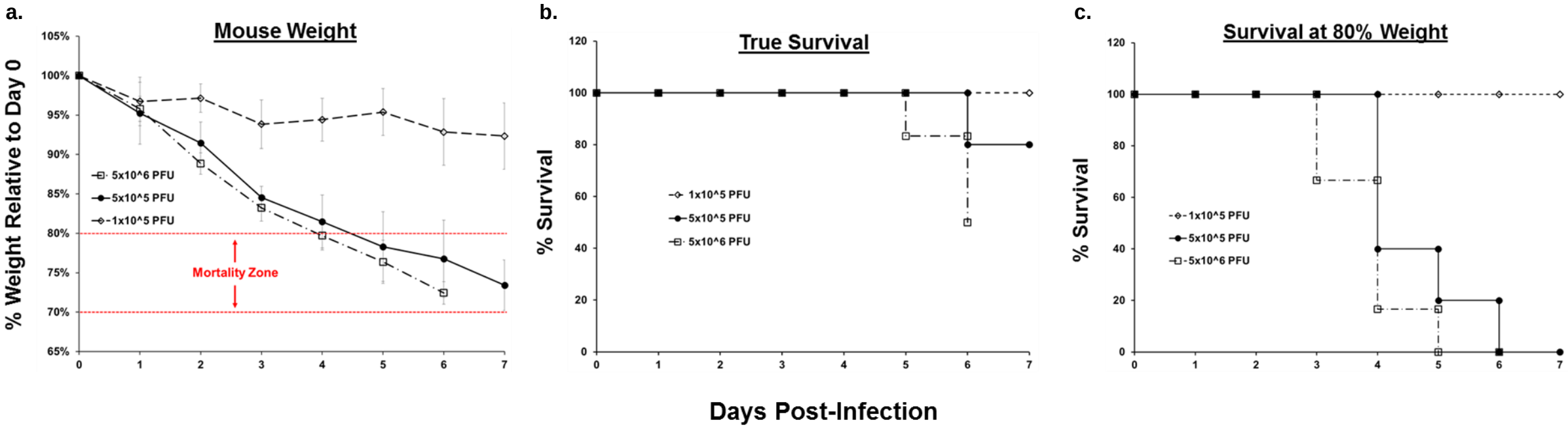

Supplementary Figure 10. An infectious clone generated with all the changes in the MERS-15 clone 2 recapitulates signs of disease. Infectious clone MERSma1 causes weight loss (a) and mortality (b & c) at both $5x10^6$ PFU (*n* = 6) and $5x10^5$ PFU (*n* = 5). Survival comparisons demonstrate dramatic differences between True survival (defined by death in cage) (b) compared to the standard in the field where mice are considered dead at an 80% humane weight cut-off (c). Based on 20-30% humane weight loss the mortality zone (red) is shown. Error bars are +/- SD.

Supplementary Figure 11

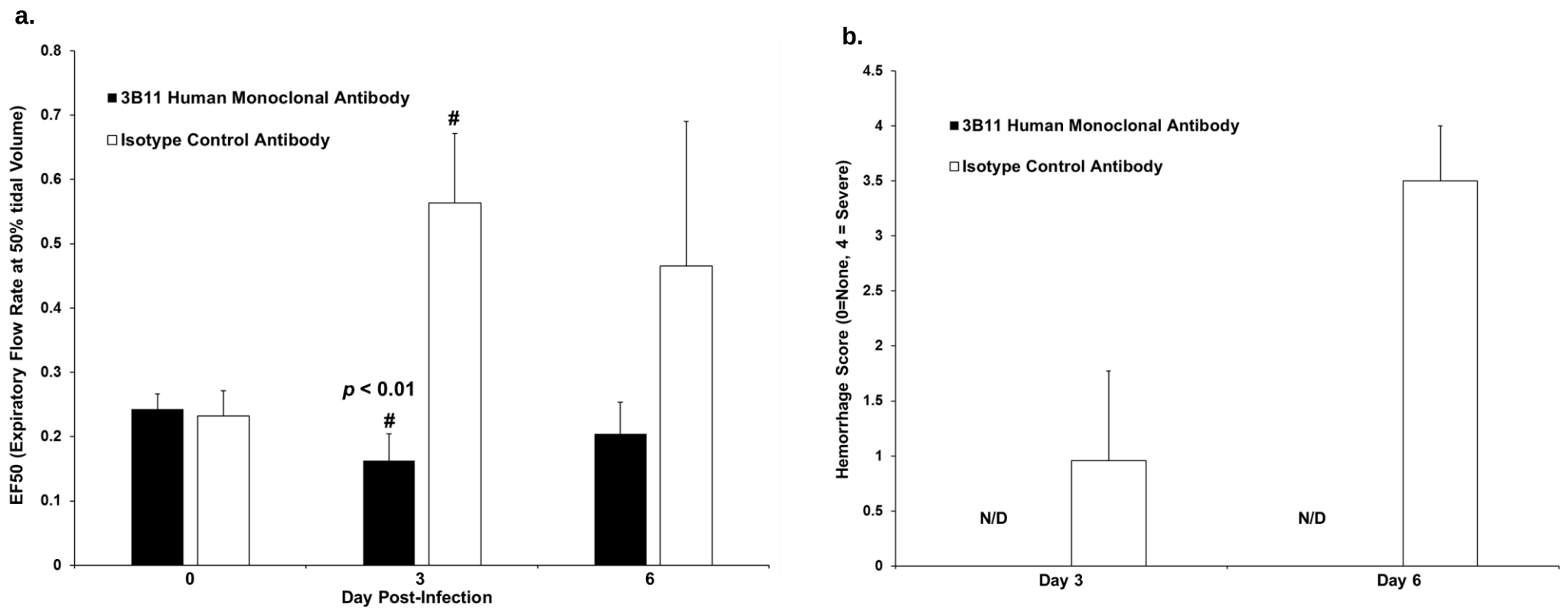

Supplementary Figure 11. 3B11 hmAB protects 288-330$^{+/+}$ mice from loss of respiratory function and hemorrhage. (a) Lung function was assessed by measuring expiratory flow rate at 50% tidal volume (EF50) at 0, 3, and 6 days p.i. for mice receiving 3B11 (day 0, 3, and 6, *n* = 6) or isotype control antibody (days 0 and 3, *n* = 6, day 6, *n* = 3). Data are represented as averages of the lung parameter measured +SD. Student *t*-test was used to compare lung function of mice receiving 3B11 human monoclonal antibody with the isotype control antibody at day 3 (# is $p < 0.01$) post-infection. (b) Lung hemorrhage was scored for mice administered 3B11 (days 3 and 6, *n* = 6) and isotype control antibody (day 3, *n* = 6 and day 6, *n* = 6) at days 3 and 6 p.i. Lungs were given a score from 0 (no hemorrhage) to 4 (severe hemorrhaging in all lobes of the lung). There was no detectable (N/D) hemorrhaging for mice receiving 3B11 human monoclonal antibody. Error bars are +SD.

Supplementary Figure 12

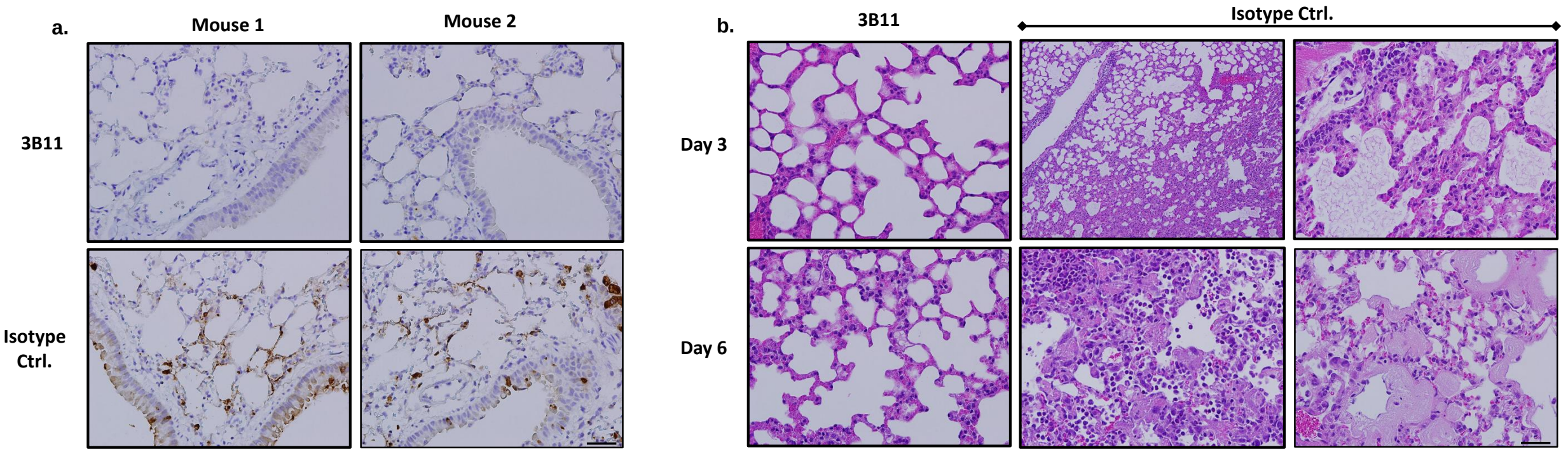

Supplementary Figure 12. 3B11 human monoclonal antibody protects from MERS-CoV-induced lung pathology. (a) IHC of lung sections at 3 days post-challenge from two different mice, treated with either 3B11 or isotype control antibodies. Infected cells are identified by IHC using anti-MERS nucleocapsid serum. (b) Pathology of lungs from 288-330$^{+/+}$ mice infected with MERS-15 C2 was assessed by H&E at days 3 and 6 post-infection. Images demonstrate severe inflammation, edema, and hyaline membrane formation in mice treated with the isotype control antibody, but absent in mice that received 3B11 hmAB. All images are at 10X or 40X magnification. Images are representative of at least 3 samples. Scale bars in lower right panels are 1mm.

Supplementary Figure 13

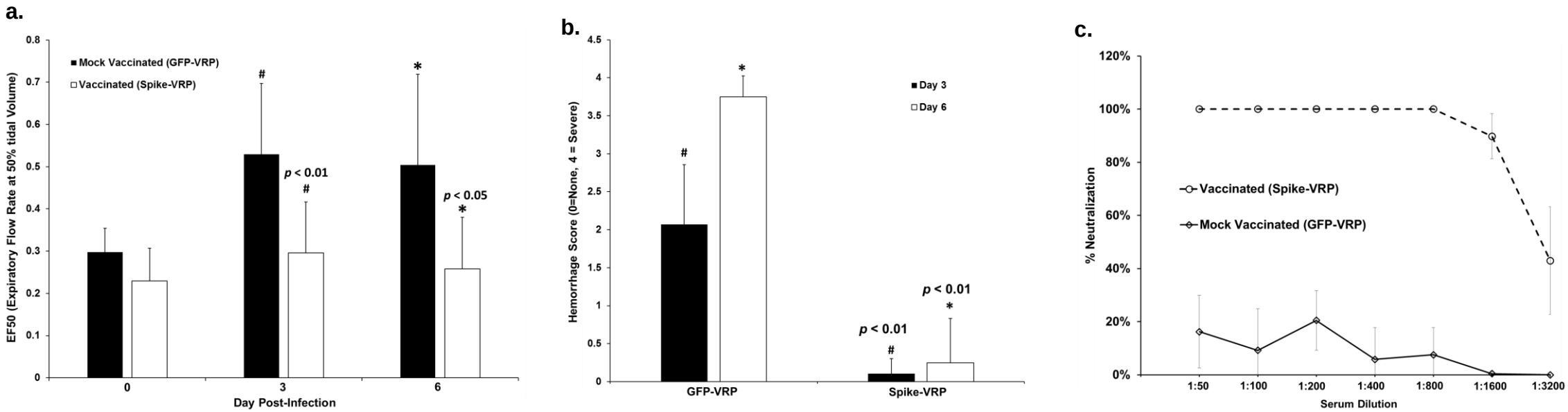

Supplementary Figure 13. Spike-VRP vaccination protects 288-330$^{+/+}$ mice. (a) Lung function was assessed by EF50 at 0, 3, and 6 days p.i. for mice receiving either GFP-VRP (days 0 and 3, *n* = 12 and day 6, *n* = 6) or Spike-VRP (days 0, 3, and 6, *n* = 12). Error bars are +SD. Student *t*-test was used to compare lung function of mice receiving GFP-VRP with Spike-VRP at day 3 (# is $p < 0.01$) and day 6 (* is $p < 0.05$) p.i. (b) Lung hemorrhage was scored for mice vaccinated with GFP-VRP (day 3, *n* = 7 and day 6, *n* = 6) or Spike-VRP (day 3, *n* = 7 and day 6, *n* = 12) at day 3 and day 6 p.i. Student *t*-test was used to compare lung hemorrhaging of mice receiving GFP-VRP with Spike-VRP at day 3 (# is $p < 0.01$) and day 6 (* is $p < 0.01$) p.i. Error bars are +SD. (c) Neutralization of MERS-15 C2 was analyzed using pre-challenge serum from spike-VRP (*n* = 5) vaccinated and GFP-VRP (*n* = 5) mock vaccinated mice. Neutralization was assessed at 2-fold dilutions within the range of 1:50 – 1:3200. Percent neutralization is indicated +/- SD.

Supplementary Figure 14

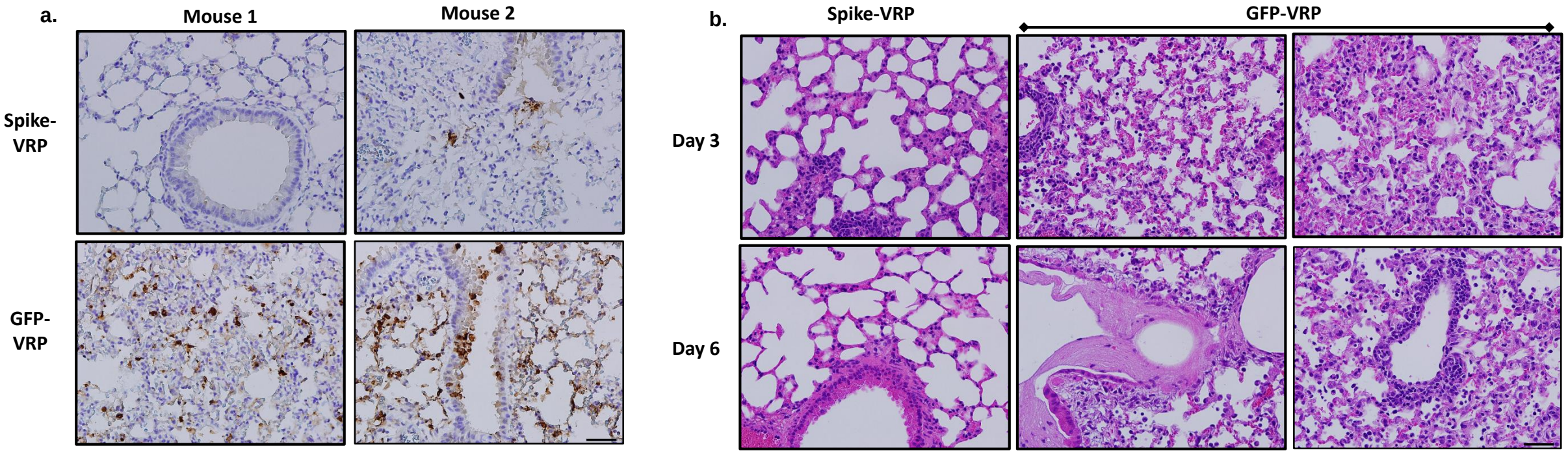

Supplementary Figure 14. Spike-VRP vaccination protects from MERS-CoV-induced lung pathology. (a) IHC of lung sections at 3 days post-challenge from two different mice. Infected cells are identified by IHC using anti-MERS nucleocapsid serum. (b) Pathology of lungs from 288-330$^{+/+}$ mice infected with MERS-15 C2 was assessed by H&E at days 3 and 6 post-infection. Images demonstrate severe inflammation, perivascular cuffing, and hyaline membrane formation only in mice that received GFP-VRP control. All images are at 40X magnification. Images are representative of at least 3 samples. Scale bars in lower right panels are 1mm.